Composites Part B 111 (2017) 348–356

Contents lists available at ScienceDirect

Composites Part B

journal homepage: www.elsevier.com/locate/compositesb

Design and characterisation of high performance, pseudo-ductile all-carbon/epoxy unidirectional hybrid composites

Gergely Czél [a, b, *], Meisam Jalalvand [b], Michael R. Wisnom [b], Tibor Czigány [a, c]

[a] MTA–BME Research Group for Composite Science and Technology, Budapest University of Technology and Economics, Műegyetem rkp. 3, H-1111 Budapest, Hungary
[b] Advanced Composites Centre for Innovation and Science, University of Bristol, Queen's Building, BS8 1TR Bristol, United Kingdom
[c] Department of Polymer Engineering, Faculty of Mechanical Engineering, Budapest University of Technology and Economics, Műegyetem rkp. 3, H-1111 Budapest, Hungary

ARTICLE INFO

Article history:
Received 6 August 2016
Received in revised form
17 November 2016
Accepted 20 November 2016
Available online 22 November 2016

Keywords:
Carbon fibre
Fragmentation
Delamination
Mechanical testing
Pseudo-ductility

ABSTRACT

A variety of thin-ply pseudo-ductile unidirectional interlayer hybrid composite materials comprising high modulus and high strength thin carbon fibre/epoxy prepregs was investigated. The central high modulus carbon plies fragmented and delaminated stably from the outer high strength carbon layers under uniaxial tensile loading in the hybrid materials. These pseudo-ductility mechanisms resulted in favourable, metal-like stress-strain responses featuring pseudo-yielding, a stress plateau and further rise in stress before final failure. The high initial elastic modulus of up to 240 GPa, the early warning and the wide safety margin between damage initiation and final failure make the new hybrids advantageous for safety-critical applications where ultimate performance and low density are key design drivers. A hybrid effect with an increase in the failure strain of the high modulus carbon material was highlighted for very thin plies.

1. Introduction

Carbon fibre/epoxy composites offer high stiffness and low density resulting in some of the highest achievable specific elastic moduli and tensile strengths among structural materials. These desirable properties make them suitable for applications such as aero-structures, spacecraft, motorsports, high specification sports equipment, where ultimate mechanical performance and lowest possible weight are crucial. Besides their high strength, carbon/epoxy composites generally exhibit unfavourable sudden and brittle failure without sufficient warning and residual integrity, which currently limits their use in many high-volume and safety-critical applications such as mass-produced automotive and construction, therefore improvements are required. The sudden failure characteristic of fibre reinforced composites is usually compensated for by conservative design limits, which hinders component manufacturers from fully exploiting their excellent mechanical properties. The possibility of creating pseudo-ductile carbon fibre reinforced composites assuring safe, progressive failure mechanisms similar to metals' yielding and strain hardening with detectable warning and a wide margin between damage initiation and final failure is therefore of high interest.

The most obvious approach to add ductility to fibre reinforced composites is to replace their intrinsically brittle constituents (i.e. glass, carbon fibres and thermosetting polymer resins) with new, more ductile materials, but the choice of suitable materials is very limited. The focus has been on fibre development as the properties of high performance composites are usually fibre-dominated. Although there are promising new materials such as nanotube fibres [1], the development to make them suitable for structural applications is extremely challenging and their verification and commercialisation is a long process. Low diameter stainless steel fibres with tensile failure strains well beyond 10% were also investigated recently as a new reinforcement for ductile composites with various matrix materials by Allaer et al. [2] and Callens et al. [3–5]. Excellent ductility was reported although the density of the obtained composites was at least twice as high as that of carbon/epoxy, which renders them less suitable for lightweight applications.

* Corresponding author. MTA-BME Research Group for Composite Science and Technology, Budapest University of Technology and Economics, Műegyetem rkp. 3, H-1111 Budapest, Hungary
E-mail address: czel@pt.bme.hu (G. Czél).

http://dx.doi.org/10.1016/j.compositesb.2016.11.049
1359-8368/

Architecture modification of laminated composites made of traditional constituents to generate additional strain using different ductility mechanisms is an alternative approach offering improvements in a shorter time scale. The additional strain can be realised e.g. by realignment of off-axis fibres and shearing of the matrix [6] [7], or from excess length due to out of plane waviness [8]. Interface modification on the fibre [9] [10], and on the ply level [11] as well as designed discontinuities [12–14] are also suitable for delaying fracture and generating stress-strain non-linearity through controlled damage before final failure.

Hybridisation of commercially available fibres is an established approach to increase the initial modulus of the high strain component and potentially introduce a gradual failure, although it usually results in an unfavourable major load drop when the low strain constituent breaks. Our intention is to use various high stiffness (low failure strain) and high strain (lower stiffness) carbon fibre/epoxy prepregs in thin format to address this issue and fully exploit the benefits of hybridisation for progressive, pseudo-ductile failure. The extensive literature on hybrid composites accumulated since the early 1970s is summarised in a few reviews [15–20]. The most practical approach based on the literature is the layer-by-layer or interlayer hybridisation, as intimate mixing of individual continuous fibres (also called intermingling) is not feasible on an industrial scale at the moment. However excellent intermingling and pseudo-ductility was presented recently with aligned discontinuous fibres [21], [22]. The vast majority of the works presenting mechanical test results of hybrid composites deal with the typical combination of continuous glass and carbon fibres to improve the relatively low failure strain and brittle fracture of carbon fibre composites. A load drop at the low strain component failure and a significant improvement in the carbon component failure strain-usually referred to as a “hybrid effect”- has generally been reported. Different aspects of the hybrid effect are extensively discussed in Refs. [20] and [23]. The importance of the correct baseline for carbon layer strain improvement was also emphasised in Ref. [23].

The authors recently demonstrated desirable stable pseudo-ductile failure in tension by hybridising uni-directional (UD) standard thickness glass and thin carbon prepreg plies [24], [25], exploiting the fragmentation and stable delamination of the carbon layer. Up to 170% increase of the baseline glass composite modulus and 2.6% pseudo-ductile strain (defined between the final failure strain and the strain on the extrapolated initial slope line at the failure stress, see Table 4) was achieved. A design framework for the hybrids was also developed in the form of both numerical [26] and analytical tools [27], [28]. These glass/carbon hybrids comprised some of the recently introduced thin-ply carbon prepregs which have generated high interest and have been studied extensively on their own [29–36] because of their unique potential to allow for highly dispersed lay-up designs resulting in favourable damage suppression properties.

There are only a few studies in the literature reporting the mechanical behaviour of hybrid composites made of different types of carbon fibres which will be referred to as all-carbon hybrids in this manuscript. Curtis and Browne [37] proposed a hybrid composite architecture where higher performance carbon fibres (T800) are put in the directions in which high stresses are expected (primary direction), and cheaper, lower performance carbon fibres (T300) are utilised in the less important directions (secondary direction). Up to 20% cost saving was anticipated while the mechanical properties of the hybrid composites were maintained at almost the same level as that of the high performance fibre reinforced baseline composites. Naito et al. [38] studied UD interlayer hybrids made of standard thickness (around 0.14 mm) prepreg plies of high strength (HS) and ultra-high modulus (UHM) carbon fibre/epoxy composites. A major load drop at the low strain component fracture was reported for hybrids with approximately 50 vol% of both components, with some load carrying capacity retained. The interlaminar fracture properties of the composites were also examined using specimens with pre-cut UHM carbon plies and release film of various lengths around the cuts. Montagnier and Hochard [39] considered high modulus (HM) and HS carbon reinforced composites for their design study of a drive shaft system. It was concluded that a hybrid composite design may reduce the number of shafts in the complete system and the total weight of the examined helicopter tail rotor driveline. Tsampas et al. [40] studied the compression performance of HS and intermediate modulus (IM) carbon hybrids in a quasi-isotropic lay-up sequence by utilising different types of prepreg plies in specific directions. No clear effect of the hybridisation on the failure loads was identified. Amacher et al., [41] and Czél et al. [42] both presented initial results at the same conference showing pseudo-ductility in quasi-isotropic hybrid laminates made of different types of carbon/epoxy. Different fibre types and stacking sequences were investigated by the two groups and both strategies yielded interesting material behaviours.

The aim of this research is to demonstrate that pseudo-ductility can be achieved with all-carbon hybrids to generate high stiffness composites exhibiting gradual failure. This will allow for high specific stiffness by a large increase in the elastic modulus and a significant decrease of the density of the new pseudo-ductile hybrid composites compared to existing glass/carbon ones. The developed materials may be suitable for some of the most demanding safety-critical applications such as aerospace, motorsports and pressure vessels where ultimate stiffness and low weight are key design drivers.

2. Material and configuration design

This section gives details of the overall concept, the applied materials and the design considerations to assure a stable pseudo-ductile failure of the hybrid laminates.

2.1. Concept

The basic concept behind pseudo-ductility in thin-ply UD interlayer hybrid composites is the exploitation of two damage mechanisms i.e. *fragmentation* of the low strain material (LSM) and dispersed, *stable delamination* or *stable pull-out* of the LSM from the high strain material (HSM) layers local to the LSM cracks as presented earlier in Refs. [24], [28]. Fragmentation in this paper refers to the damage process where multiple fractures take place stably in a UD composite ply or layer loaded in tension parallel to the fibres. The fractures in the carbon plies were observed earlier [24] in UD glass/carbon hybrids visually through the translucent glass plies, which is not possible in the all-carbon/epoxy composites. It can be detected here as an almost horizontal plateau in the stress/strain response, when more and more fractures take place in the LSM upon further increase of displacement accompanied by only a small increase in stress. The fragmentation of the LSM is only achievable if the energy release rate at first LSM fracture is lower than the mode II fracture toughness of the interface between the LSM and HSM layers so that global unstable delamination of the layers is prevented. Instead, delamination may either be completely absent, or present in a dispersed, stable, localised form due to the low energy available to drive it. Therefore thin constituent prepregs are utilised to limit the energy released at the first LSM fracture. The resulting expected stress-strain responses of the studied UD hybrids are given in Fig. 1. The key features of the expected response are a quasi-linear initial part, a flat, wide stress plateau and a second rising part before final failure. This metal-like failure character

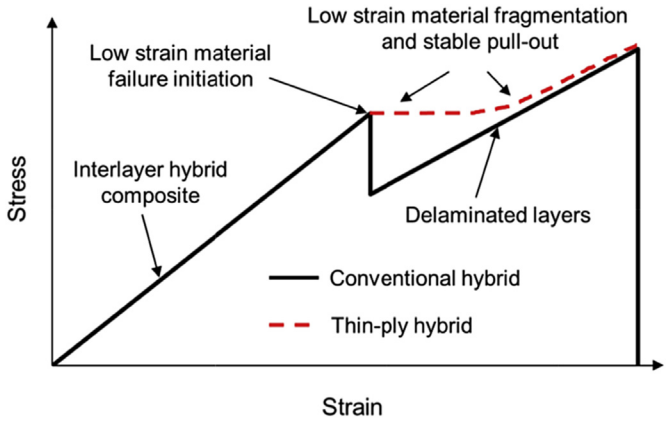

Fig. 1. Schematic of the stress-strain response of conventional and thin-ply interlayer hybrid composites.

assures a warning sign which can be easily detected e.g. by acoustic emission [43] and provides a significant stress and strain margin after the first fracture of the LSM layer. These are large improvements to the brittle failure of conventional UD composites. In this study the previously demonstrated thin-ply hybrid concept is applied to all-carbon hybrids.

2.2. Materials

The materials considered for design, and used for the experiments were thin carbon/epoxy prepregs from North Thin Ply Technology made of different type intermediate modulus (IM), high modulus (HM) and ultra-high modulus (UHM) carbon fibres. The choice of fibres in the utilised prepregs was driven by a previous parametric study [28] revealing that the higher the difference between the moduli of the hybridised materials, the larger the pseudo-ductile strain that may be achieved. This is the main reason for hybridising IM carbon fibres with HM and UHM carbon fibres. The matrix in all utilised prepregs was North TPT's ThinPreg 120 EPHTg- 402 a 120 °C cure toughened epoxy. Basic properties of the applied fibres and prepreg systems can be found in Tables 1 and 2. Please note, that the volume fraction of the thin prepregs were about 50%, 10 absolute% lower than that of standard thickness high performance composites, which limits the maximum achievable stiffness of the developed pseudo-ductile configurations.

2.3. Design of hybrid laminates

The following design criteria were identified earlier [24] to assure stable pseudo-ductile failure for UD glass/carbon interlayer hybrids. These criteria were adopted here for the preliminary design of similar interlayer hybrid configurations with new sets of constituent prepregs:

(i) The outer, HSM layers (see Fig. 3) need to be thick and strong enough to take the full load after low strain material fracture and pull-out. A sufficient margin should also be allowed to account for stress concentration in the HSM layer due to the LSM layer fracture which was not initially considered in this approach, but was shown not to be a major effect for similar interlayer hybrid configurations [27]. Inequality (1) is useful for choosing the high strain constituent material and gives the minimum strength of the HSM layer for given layer thicknesses and initial moduli.

$$\sigma_{1b} > \frac{\sigma_{2b}(2E_1t_1 + E_2t_2)}{2E_2t_1} \tag{1}$$

where E_1 is the initial modulus of the HSM layers, E_2 is the initial modulus of the LSM layer, t_1 is the thickness of one HSM layer, t_2 is the thickness of the LSM layer as shown on Fig. 3, σ_{1b} is the breaking stress of the HSM layers, σ_{2b} is the breaking stress of the LSM layer.

Inequality (1) can be rearranged in another form which is more practical for stacking sequence design. Inequality (2) gives the minimum thickness of one HSM layer for a given material pair and LSM thickness required to avoid premature failure at LSM layer fracture.

$$t_1 > \frac{\varepsilon_{2b}E_2t_2}{2E_1(\varepsilon_{1b} - \varepsilon_{2b})} \tag{2}$$

Table 1
Fibre properties of the applied UD prepregs based on manufacturer's data (Numbers in brackets indicate the tow count in 1000 filaments. IM-intermediate modulus, HM-high modulus, UHM-ultra-high modulus).

Carbon fibre type	Fibre manufacturer	Elastic modulus [GPa]	Strain to failure [%]	Tensile strength [GPa]	Density [g/cm^3]	Coefficient of thermal expansion 10^{-6} [1/°C]
Torayca T1000GB (12k)	Toray	294 (IM)	2.2	6.37	1.80	−0.55
Torayca M55JB (6k)	Toray	540 (HM)	0.8	4.02	1.91	−1.1
Granoc YSH-70A (6k)	Nippon GFC	720 (UHM)	0.5	3.63	2.15	−1.5
Granoc XN-80 (12k)	Nippon GFC	780 (UHM)	0.5	3.43	2.17	−1.5

Table 2
Cured ply properties of the applied UD prepregs (The last row shows data used for hybrid laminate design with equivalent thickness for 49.4% fibre volume fraction assuming the same modulus as for the thinner plies.).

Prepreg material	Prepreg manufacturer	Nominal fibre areal density[a] [g/m^2]	Fibre volume fraction[a] v_f [%]	Cured ply thickness[b] [μm]	Initial modulus[b] [GPa]
T1000/epoxy	North TPT	28	48.1	32.3	142.9
M55/epoxy	North TPT	30	51.3	30.8	277.1
YSH-70A/epoxy	North TPT	30	51.4	27.1	371.7
XN-80/epoxy	North TPT	50	49.4	46.7	386.7
XN-80/epoxy	North TPT	63	46.5	62.5	364.4
XN-80/epoxy	North TPT	63	49.4	58.8[c]	386.7

[a] Based on manufacturer's data.
[b] Calculated using manufacturer's data.
[c] Equivalent thickness for the same v_f as that of the 50 g/m^2 XN-80/epoxy prepreg.

Table 3
Specimen types tested (GSM-areal density in [g/m^2]. Subscripts indicating the number of plies in a block are only added where multiple plies were stacked together. LSM-low strain material. Relative LSM layer thickness was normalised by the full specimen thickness.).

Hybrid configuration (Abbreviation) [Lay-up sequence]	Fibre areal densities [g/m^2]	Nominal thickness h [mm]	Relative LSM layer thickness [–]	Calculated G_{II} at LSM failure strain[a] [N/mm]	Predicted modulus [GPa]	Thermal residual strain in LSM [%]
(M55) [T1000$_2$/M55/T1000$_2$]	56/30/56	0.160	0.192	0.199 at 0.8%	168.6	−0.0061
(YSH-70A) [T1000/YSH-70A/T1000]	28/30/28	0.092	0.295	0.132 at 0.5%	210.4	−0.0066
(50 GSM XN-80 blocked) [T1000$_2$/50 GSM XN-80$_2$/T1000$_2$]	56/100/56	0.223	0.419	0.416 at 0.4%[a]	245.0	−0.0046
(50 GSM XN-80 dispersed) [T1000/50 GSM XN-80/T1000]$_S$	(28/50/28)$_S$	2·0.112	0.419	0.213 at 0.4%	245.0	−0.0046
(63 GSM XN-80) [T1000$_2$/63 GSM XN-80/T1000$_2$]	56/63/56	0.192	0.325	0.203 at 0.4%	214.9	−0.0060

[a] LSM failure strain was assumed the same as the quoted fibre failure strain, except for XN-80 where a lower strain was used based on previous experimental results on S-glass/XN-80 interlayer hybrid specimens [25].

where ε_{1b} and ε_{2b} are the breaking strain of the HSM and LSM layers respectively. If, as a first approximation, the breaking strains are assumed to be equal to the failure strains of the fibres, a lower bound for the HSM layer thickness can be obtained.

(ii) The energy release rate (G_{II}) at the expected failure strain of the LSM layer must be lower than the mode II fracture toughness (G_{IIC}) of the interface to avoid catastrophic delamination of the central LSM layer after its first fracture. This criterion assures the condition for fragmentation and stable pull-out of the LSM layer.

$$G_{II} = \frac{\varepsilon_{2b}^2 E_2 t_2 (2E_1 t_1 + E_2 t_2)}{8E_1 t_1} < G_{IIC} \tag{3}$$

The preliminary design based on the properties of the available prepreg materials and the above criterion resulted in the configurations summarised in Table 3. The minimum required thickness of the HSM layer is exceeded in each configuration and the predicted mode II energy release rate G_{II} at LSM failure strain in all cases is significantly lower than 0.5 N/mm which is the estimated fracture toughness G_{IIC} of the tested materials. The critical value is based on observations during previous tests on similar hybrid configurations made of prepregs comprising the same epoxy matrix system [44]. A change from stable to unstable failure was observed earlier in configurations having G_{II}>0.5 N/mm therefore this value was adopted as an approximation for G_{IIC}. Based on the above discussion, all configurations are expected to fail in a progressive, pseudo-ductile way showing LSM fragmentation and stable pull-out. Two scaled configurations of T1000 and XN-80 fibres (one with blocked and one with dispersed lay-up sequence) are tested to analyse the effect of layer thicknesses and the corresponding energy release rate on the failure process. The third configuration of the same material pair was included to show the effect of the relative LSM thickness (to full thickness). The reason for testing a plate made of two identical sub-laminates in the *50 GSM XN-80 dispersed* configuration, is that this material combination was tested early in the experimental study and our design was initially cautious as it is hard to machine and handle very thin laminates. It was confirmed later when other types were tested that it is possible to handle thin laminates of less than 0.2 mm thickness.

The thermal residual strain in the LSM was calculated using the moduli of the prepregs, the 100 °C difference between cure and room temperatures, the coefficients of thermal expansion (CTE) of the fibres given in Table 1 and a typical value for the epoxy from the literature and included in Table 3 as well.

A more advanced design tool based on the analytical criteria was also applied to the available material combinations to predict the expected failure mechanisms. The so-called damage-mode maps were developed by the authors recently and full details on how to generate the maps can be found in Refs. [27], [28].

The horizontal axis of each map in Fig. 2 shows the relative LSM layer thickness with regards to the full thickness of the hybrid laminate and the vertical one shows the absolute thickness of the LSM layer so every point on the map represents a specific hybrid configuration of a given material pair. The maps show the expected damage modes and the achievable pseudo-ductile strains for the

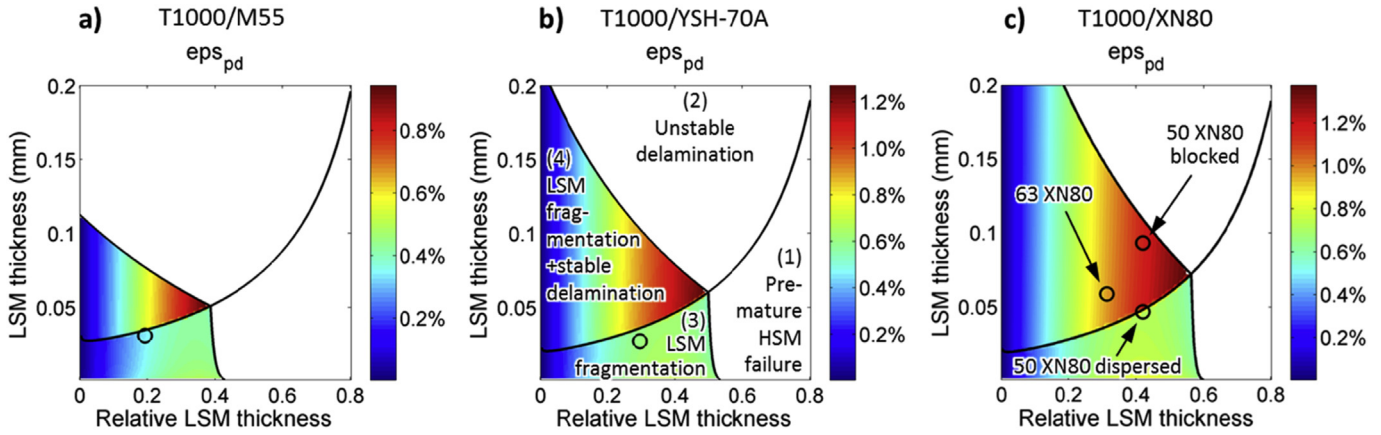

Fig. 2. Damage mode maps of the designed material combinations (eps$_{pd}$-pseudo-ductile strain represented by the colour palette, LSM-low strain material, HSM-high strain material, part b) indicates four regions of the map with their associated failure processes). (For interpretation of the references to colour in this figure legend, the reader is referred to the web version of this article.)

selected configurations marked with circles. The pseudo-ductile strain (see Table 4 for graphical definition) is a good measure of improvement in failure type against sudden catastrophic fracture of the whole hybrid laminate therefore it was selected to indicate the ductility performance of the designed material configurations. The coloured regions of the maps indicate favourable pseudo-ductile damage process and the white regions show either premature HSM layer failure or catastrophic delamination. Each damage mode map in Fig. 2 was generated with a $G_{IIC} = 0.5$ N/mm estimated fracture toughness and the first LSM layer fracture was assumed to take place at the strains used for energy release rate calculation and given in Table 3. The HSM layer failure which always leads to final failure of the hybrid laminate depends on the variation of strain along the fragment lengths and the volume of material. This was estimated using a statistical strength distribution based on a typical Weibull modulus of 30 and reference failure strain of 2.2% for a reference volume of 1 mm^3 for the T1000 plies. This approach follows the one used successfully in Ref. [27] which should give conservative design configurations. A stress concentration factor of $K_t = 1.08$ was assumed around the fractured low strain layer as explained in Ref. [27] for more accurate failure type prediction, but those at the end-tab region were not considered, therefore the predicted pseudo-ductile strains represent upper bounds.

Each map in Fig. 2 shows the expected pseudo-ductile strain of a given material combination in terms of the relative and absolute thickness of the LSM layer for all the possible configurations. The maps divide the design plane of a material pair into four regions (see Fig. 2b) associated with four possible damage sequences of UD interlayer hybrid composites i.e. (1) *Premature HSM failure*: the whole hybrid laminate fails at first LSM fracture, (2) *Unstable delamination*: the layers delaminate at first LSM fracture, (3) *LSM layer fragmentation*: the energy released at first LSM layer fracture is low enough so that unstable delamination is suppressed and other fractures can take place in the LSM layer until they saturate, (4) *LSM fragmentation and stable delamination*: the energy release rate is lower than the fracture toughness at LSM failure but exceeds that after saturation of the LSM fragmentation before final failure. Therefore the fragmented LSM segments are pulled-out stably from the HSM layers (see Fig. 1).

Only one map was generated for T1000/XN-80 hybrids, where $v_f = 49.4\%$ was used for both thickness XN-80 prepregs. A reduced equivalent thickness was calculated for the lower volume fraction 63 g/m^2 XN-80 prepreg type as shown in Table 2 keeping the ply stiffness constant. The damage mode maps predict pseudo-ductile failure for all five designed configurations. Three of them fall into the *LSM fragmentation only* region, but they are very close to the boundary of *LSM fragmentation and stable delamination* region where the remaining two configurations sit and where the best pseudo-ductile properties are achievable. Please note that more optimal design was hindered by the limited choice of available thin carbon/epoxy prepregs (e.g. layer thicknesses in the hybrids were governed by available ply thicknesses). The designed configurations were deemed safe enough against premature or unstable failure and they were promising desirable properties despite the limitations and therefore they were all manufactured and tested. The damage mode maps proved to be powerful tools to design optimal hybrids laminates with desired behaviour and to predict the failure mode of a given configuration.

3. Experimental

3.1. Specimen geometry

The specimens tested within the study were UD, parallel edge end-tabbed tensile specimens. Nominal specimen dimensions were

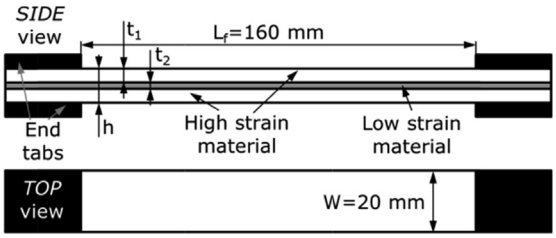

Fig. 3. Schematic of the specimen geometry.

240/160/20/*h* mm overall length/L_f -free length/*W*-width/*h*-variable thickness respectively. Fig. 3 shows the geometric parameters on the side and top view schematics of a tensile specimen.

3.2. Specimen manufacturing

The interlayer hybrid specimens were made by stacking the specified prepreg layers on top of each other, vacuum bagging the composite plate and curing it in an autoclave according to the recommended cure cycle of the constituent prepregs (2 h at 120 °C and 0.7 MPa pressure). The individual specimens were cut from 300 × 300 mm plates with a diamond cutting wheel in the case of specimens thicker than 0.2 mm and thinner laminates were cut with a CNC laser cutter. The edges of specimens cut with the laser were finished with P240 grit size sandpaper on a flat board. Finally 40 mm long, 2 mm thick cross-ply glass/epoxy tabs were bonded to the ends of the specimens with a two component epoxy adhesive.

3.3. Test method

Testing of the parallel edge specimens was executed under uniaxial tensile loading and displacement control at a crosshead speed of 2 mm/min on a computer controlled Instron 8801 type 100 kN rated universal hydraulic test machine with a regularly calibrated 25 kN load cell and wedge type hydraulic grips. The grip pressure was kept at the minimum required to avoid slippage of the specimens in the grips during loading to minimise the through thickness compressive stress at the end of the specimens. Strains were measured using an Imetrum video extensometer, with a nominal gauge length of 130 mm. A minimum of five specimens were tested from each configuration.

3.4. Results and discussion

Fig. 4 shows the stress-strain response of the *M55* configuration comprising HM carbon fibres in the central LSM layer. The curves show smooth transitions between the initial linear part, the short, slightly rising plateau corresponding to fragmentation and the second linear part. The plateau indicates that the LSM layer fragmented progressively and the absence of any load-drop implies that there was no catastrophic delamination of the LSM from the HSM. The rounded knees between the first and second straight sections are likely formed because of the low energy release rate at LSM failure and hence low probability of stable delamination, as predicted by the corresponding damage mode map (see Fig. 2a). This can result in a dispersed spatial distribution of initiating damage with several small cracks growing slowly at the same time while the stiffness of the hybrid is gradually reduced. The shape of the curves confirms the fragmentation of the LSM layer (plateau region) and gives the desired warning through sub-critical damage accumulation that is detectable e.g. by acoustic emission [43] or stiffness monitoring before final failure. The stress at damage initiation (first knee of the curves) was 1400 MPa on average which is high compared to other pseudo-ductile composites (around

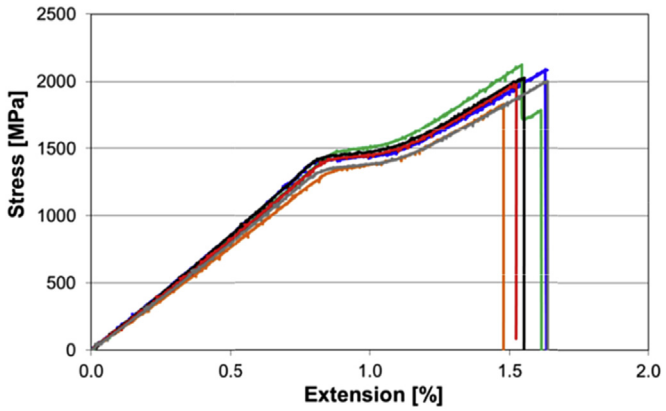

Fig. 4. Tensile response of the *M55* configuration.

1000 MPa for UD glass/carbon [25]) or ductile metals.

Fig. 5 shows the stress-strain curves of the *YSH-70A* configuration. Smooth transitions and a very stable pseudo-ductile response were achieved in agreement with the prediction of the damage mode map and the very low energy release rate of this configuration primarily due to its very low thickness. A high initial modulus around 200 GPa was achieved which exceeds the stiffness of intermediate modulus (IM) carbon/epoxy composites of higher fibre volume fraction than that of the materials tested here. It is interesting to note, that the pseudo-yield strain of this hybrid -defined by the intersection of lines fitted to the initial linear and the plateau part of the stress-strain curves (see Table 4.)- was 0.58%, significantly higher than 0.5% which is given in the manufacturer's data sheet for the YSH-70A fibres. This indicates that there may be a hybrid effect increasing the LSM layer failure strain in this configuration because the development of broken fibre clusters could have been delayed by the low thickness of the LSM ply in the centre of the hybrid laminate. The LSM fibre failure strain given by the manufacturer is however not a satisfactory baseline to claim a hybrid effect. The importance of the LSM baseline strain and the types of possible hybrid effects are discussed extensively in Ref. [23].

Fig. 6 shows the stress-strain response of three different configurations made of XN-80 and T1000 fibres. All configurations exhibited excellent pseudo-ductility with high initial moduli of up to 250 GPa and wide margins between damage initiation (first knee in the curves) and final failure which can serve as an intrinsic warning sign of overloading. The baseline design of *50 GSM XN-80 blocked* type hybrid is built up of the thickest block of the LSM and has the highest energy release rate which is still sub-critical, therefore the LSM layer fragmented (a flat stress plateau was present in the stress strain graph) and a favourable failure process was obtained. The small stress fluctuations over the plateau strain regime indicate dispersed local delaminations around the LSM fractures corresponding to stable pull-out of the LSM fragments from the HSM plies. The pseudo-ductile strain of this configuration was the highest (up to 0.94%) in reasonable agreement (see Table 4) with the prediction of the corresponding damage mode map (Fig. 2c) indicating LSM fragmentation and stable delamination. The deviation in the predicted and measured pseudo-ductile strains is mostly attributed to the stress concentrations around the end-tabs affecting the final failure strain of the hybrids by HSM fracture. This effect was not implemented in the damage mode maps but could cause premature failure of the hybrids.

The second *50 GSM XN-80 dispersed* configuration has two sub-laminates of hybrid blocks with half the thickness of the blocked type. This means that the *relative LSM thickness* of the *dispersed* and the *blocked* configurations is the same but the absolute thickness of the hybrid sub-laminates as well as the LSM layer is halved (see Fig. 2c). The thinner hybrid blocks of the *dispersed* type resulted in only half the amount of energy released at LSM fracture than in case of the *blocked* configuration (see Table 3). The pseudo-ductile strain of this configuration was limited by the early final failure which was most probably due to high stress concentrations around LSM layer fractures caused by the predicted low probability for stable pull-out capable of releasing the stress-concentrations (see Fig. 2c). This explanation is based on earlier numerical analysis of the effect of LSM absolute thickness on the stress concentration around LSM cracks in scaled UD glass/carbon hybrid laminates discussed in Ref. [26]. It was also reported elsewhere by the authors [23], that the thickness of the LSM layer has a significant effect on the damage initiation strain of the interlayer hybrids, because the development of broken fibre clusters is limited by the actual layer thickness. This so-called initiation hybrid effect is clearly present in the two scaled configurations of *50 GSM XN-80 blocked* and *dispersed*. A consistent increase of the pseudo-yield strain was observed in Fig. 6 from 0.398% to 0.422% just by using two half thickness sub-laminates of the same materials instead of thicker blocks. A two-sample Student's t-test indicated that the expected values of the pseudo-yield strains of the *50 GSM XN-80 blocked* and *dispersed* configurations are different at a 97% probability level.

The third *63 GSM XN-80* configuration had only a slightly lower energy release rate than the *dispersed* one and therefore is suitable

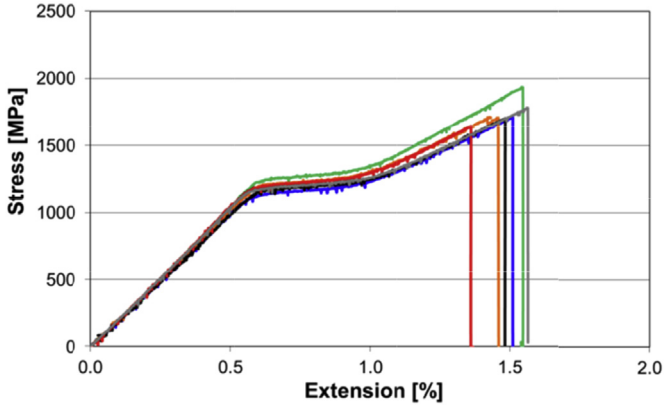

Fig. 5. Tensile response of the *YSH-70A* configuration.

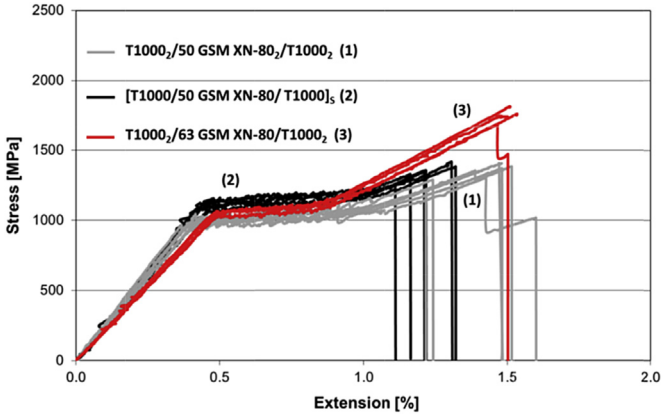

Fig. 6. Tensile response of T1000/XN-80 configurations (GSM refers to the areal density of the constituent prepregs in [g/m^2]).

to highlight the effect of the different *relative LSM thickness* (see Fig. 2c), which is most obvious from the lower initial modulus. Since the LSM ratio was less in this configuration than in the others, the length of the plateau and the change between initial and final slope of the stress-strain curves –corresponding to the contribution of the LSM layer to the hybrid stiffness-was lower. Although the energy release rate of this configuration at 0.4% strain was lower than that of the *dispersed* type, this hybrid was more likely to delaminate stably due to its higher HSM thickness, which could withstand stress-concentrations until higher strains at which stable pull-out took place. The obtained pseudo-ductile strain value was well predicted by the damage mode maps and it was in between that of the other two configurations of the same materials. It was noted that this type had the highest pseudo-yield strain of all XN80 configurations. This may have been caused by less damage introduced to the 63 g/m^2 XN80 prepreg when it was spread compared with the thinner 50 g/m^2 type. More stable stress-strain traces of the *63 GSM XN-80* specimens confirm that there may have been a wider margin between the actual and the critical energy release rates in this configuration than in others.

Table 4 summarises the results of the tested configurations and gives the definitions of the pseudo-ductility parameters. The initial modulus values were evaluated with the nominal thicknesses based on assuming constant fibre areal densities and fibre volume fractions to exclude the effect of thickness variation due to small variations in resin distribution (see Table 3). The pseudo-yield points were evaluated at each individual specimen's stress-strain curve at the intersection of lines fitted to the initial linear and the plateau parts of the curves and the average pseudo-ductile strains were determined graphically by fitting lines to the aggregated test graphs of each series. It is worth noting that the pseudo-yield strain of the *50 GSM XN-80 blocked* configuration was only 0.4%, similar to the value obtained earlier in Ref. [25] for the same thickness XN-80/epoxy block in S-glass/epoxy. The higher pseudo-yield strain of the *50 GSM XN-80 dispersed* configuration is attributed to a hybrid effect due to the lower LSM thickness. In the case of the *63 GSM XN-80* type, the pseudo-yield strain could have been higher due to less damage introduced to the thicker XN80 prepreg during the tow spreading process. However, the fibre damage in different thickness thin plies and its effect on ply failure was not investigated therefore this hypothesis could not be confirmed. The pseudo-yield strains of the *M55* and the *YSH-70A* types both exceed the strain of the LSM fibres given by the manufacturer, which could be attributed to a hybrid effect due to low thickness as well, but we do not have sufficient baseline LSM strains to claim this with confidence. The table reveals that the final failure strains of all hybrid configurations are significantly lower than the quoted failure strain of the T1000 carbon fibres in the HSM, but we have no information on how the fibre strain was measured. This effect is commonly observed in UD composites and is usually attributed to stress concentrations at the end-tabs, size effects and possible manufacturing and machining defects. Videos recorded during the tests for strain measurement confirmed that the final failure of most of the specimens from all types took place near the end-tabs. Strains to HSM failure may also have been reduced due to fibre damage during the spreading of the tows to create the very thin plies. The main reason for obtaining particularly low values of only 1.2% for the final failure strain of *50 GSM XN-80 dispersed* configuration is that this configuration was not expected to show stable LSM pull-out and therefore was susceptible to higher stress concentrations around the LSM layer

Table 4
Results summary of the specimen types tested (LSM-low strain material, relative LSM layer thickness was normalised with the full specimen thickness. Numbers in brackets indicate the coefficients of variation in [relative %].).

Spec. Type	Relative LSM layer thickness	Initial modulus	Modulus increase (to pure T1000/epoxy[a])	Pseudo-yield strain[b] ε_{py}	Pseudo-yield stress[b] σ_{py}	Final failure strain	Pseudo-ductile strain[d] ε_{pd}	Predicted pseudo-ductile strain[e]
	[-]	[GPa]	[%]	[%]	[MPa]	[%]	[%]	[%]
M55	0.192	159.9 (4.4)	11.9	0.827 (2.8)	1400.9 (3.7)	1.57 (4.1)	0.32	0.41
YSH-70A	0.295	196.1(3.1)	37.2	0.570 (2.4)	1179.6 (3.4)	1.50 (5.1)	0.62	0.72
50 GSM XN-80 blocked	0.419	244.8 (3.9)	71.3	0.398 (4.8)	989.7 (1.9)	1.46 (8.2)	0.94	1.16
50 GSM XN-80 dispersed	0.419	242.5 (4.8)	69.7	0.422 (1.6)	1065.8 (2.8)	1.21(6.7)	0.65	0.88
63 GSM XN-80	0.325	207.9 (3.0)	50.4	0.480 (1.9)	1030.3 (3.9)	1.53[c]	0.70	0.97

[a]Baseline T1000/epoxy composite modulus: 142.9 GPa (see Table 2)
[b]*Pseudo-yield points* (ε_{py}- pseudo-yield strain; σ_{py}- pseudo-yield stress) were defined as the intersection of lines fitted to the end of the quasi-linear section of the curves and the stress plateaus. Figures are corrected for thermal residual strains of the LSM.
[c]Approximate value, some of the tests stopped at first sign of failure
[d]*Pseudo-ductile strain* (ε_{pd}) was defined between the strain of a point on the initial slope line at the *failure stress* and the *strain at the failure stress*. Figures were determined graphically from lines fitted to the aggregated test curves of each test series.
[e]Predicted by the damage mode maps

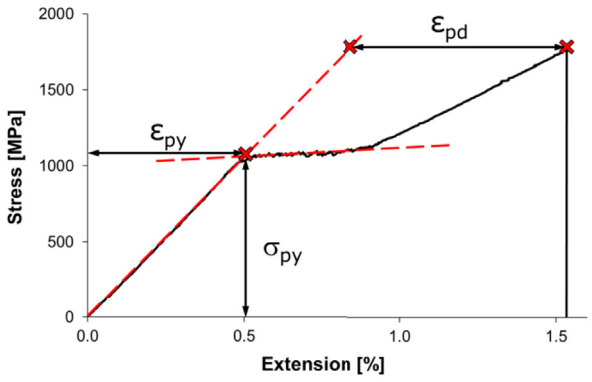

fractures. Another reason for early final failure is that single plies of the thin T1000 HSM may not result in a complete cover of the specimen due to small gaps between the tows in the prepreg observed during lay-up. These defects may have induced weak spots and initiated premature failure around the end tabs where multiple stress concentrations are also present (end-tab effect and stress concentration at the edge of LSM fragments). The probability of stable delamination capable of reducing stress-concentrations was predicted to be significantly increased, while the probability of uncovered spots was reduced by utilising double T1000 HSM plies in the other two T1000/XN-80 configurations, finally resulting in higher final failure strains of around 1.5%.

4. Conclusions

The following conclusions were drawn from the study of thin-ply unidirectional all-carbon/epoxy interlayer hybrid composites:

- A series of new high performance, unidirectional all-carbon/epoxy interlayer hybrid configurations were presented. Pseudo-ductility was demonstrated with all five tested configurations with high initial moduli providing up to 70% increase to the high strain material baseline. Well defined, wide plateaus were observed due to low strain material fragmentation which could be exploited as a warning sign before final failure if monitored e.g. by acoustic emission.
- The *M55* configuration provided high initial modulus of 160 GPa together with 0.83% pseudo-yield (i.e. damage initiation) strain and 1400 MPa pseudo-yield stress, which is the highest pseudo-yield stress we have achieved with pseudo-ductile UD hybrids so far. The *50 GSM XN-80 blocked* type material exhibited outstanding 245 GPa initial modulus, 990 MPa pseudo-yield stress and high, 0.94% pseudo-ductile strain. These figures demonstrate the wide range of properties achievable and highlight the potential to tailor the mechanical response of the proposed hybrid materials.
- The scaled configurations of *50 GSM XN-80 blocked* and *dispersed* types confirmed the key role of the low strain material layer thickness in controlling the hybrid effect in the unidirectional all-carbon/epoxy hybrid material.
- Good agreement was achieved between predicted and experimentally observed failure modes of the unidirectional carbon/epoxy interlayer hybrid composites. The predictions for the pseudo-ductile strains were reasonable. The presented study validated the damage mode map approach with a new set of materials and highlighted its merit for design and prediction.

Acknowledgement

This work was funded under the UK Engineering and Physical Sciences Research Council Programme Grant EP/I02946X/1 on High Performance Ductile Composite Technology in collaboration with Imperial College London. Gergely Czél acknowledges the Hungarian Academy of Sciences for funding through the Post-Doctoral Researcher Programme fellowship scheme, the János Bolyai scholarship and the Hungarian National Research, Development and Innovation Office - NKFIH for funding through grant ref. OTKA K 116070 and OTKA PD 121121. The authors acknowledge Tamás Rév for his help with some of the experiments and North TPT for supplying materials for this research. All data required for reproducibility are provided within the paper.

References

[1] Boncel S, Rajyashree M, Sundaram RM, Windle AH, Koziol KKK. Enhancement of the mechanical properties of directly spun CNT fibers by chemical treatment. ACS Nano 2011;5:9339–44.
[2] Allaer K, De Baere I, Lava P, Van Paepegem W, Degrieck J. On the in-plane mechanical properties of stainless steel fibre reinforced ductile composites. Compos Sci Technol 2014;100:34–43.
[3] Callens MG, Gorbatikh L, Verpoest I. Ductile steel fibre composites with brittle and ductile matrices. Compos Part A Appl Sci Manuf 2014;61:235–44.
[4] Callens MG, Gorbatikh L, Bertels E, Goderis B, Smet M, Verpoest I. Tensile behaviour of stainless steel fibre/epoxy composites with modified adhesion. Compos Part A Appl Sci Manuf 2015;69:208–18.
[5] Callens MG, De Cuyper P, Gorbatikh L, Verpoest I. Effect of fibre architecture on the tensile and impact behaviour of ductile stainless steel fibre polypropylene composites. Compos Struct 2015;119:528–33.
[6] Fuller JD, Wisnom MR. Pseudo-ductility and damage suppression in thin ply CFRP angle-ply laminates. Compos Part A Appl Sci Manuf 2015;69:64–71.
[7] Fuller JD, Wisnom MR. Exploration of the potential for pseudo-ductility in thin ply CFRP angle-ply laminates via an analytical method. Compos Sci Technol 2015;112:8–15.
[8] Pimenta S, Robinson P. Wavy-ply sandwich with composite skins and crushable core for ductility and energy absorption. Compos Struct 2014;104:111–24.
[9] Qiana H, Bismarck A, Greenhalgh ES, Shaffer MSP. Carbon nanotube grafted carbon fibres: a study of wetting and fibre fragmentation. Compos Part A: Appl Sci Manuf 2010;41:1107–14.
[10] Asadi A, Miller M, Moon RJ, Kalaitzidou K. Improving the interfacial and mechanical properties of short glass fiber/epoxy composites by coating the glass fibers with cellulose nanocrystals. Express Polym Lett 2016;10:587–97.
[11] Grail G, Pimenta S, Pinho ST, Robinson P. Exploring the potential of interleaving to delay catastrophic failure in unidirectional composites under tensile loading. Compos Sci Technol 2015;106:100–9.
[12] Pimenta S, Robinson P. An analytical shear-lag model for composites with 'brick-and-mortar' architecture considering non-linear matrix response and failure. Compos Sci Technol 2014;104:111–24.
[13] Czel G, Pimenta S, Wisnom MR, Robinson P. Demonstration of pseudo-ductility in unidirectional discontinuous carbon fibre/epoxy prepreg composites. Compos Sci Technol 2015;106:110–9.
[14] Czél G, Jalalvand M, Wisnom MR. Demonstration of pseudo-ductility in unidirectional hybrid composites made of discontinuous carbon/epoxy and continuous glass/epoxy plies. Compos Part A Appl Sci Manuf 2015;72:75–84.
[15] Hancox NL. Fibre composite hybrid materials. London: Applied Science Publishers Ltd.; 1981.
[16] Summerscales J, Short D. Carbon fibre and glass fibre hybrid reinforced plastics. Composites 1978;9:157–66.
[17] Short D, Summerscales J. Hybrids - a review Part 1. Techniques design and construction. Composites 1979;10:215–21.
[18] Short D, Summerscales J. Hybrids - a review Part 2. Physical properties. Composites 1980;11:33–8.
[19] Kretsis G. A review of the tensile, compressive, flexural and shear properties of hybrid fibre-reinforced plastics. Composites 1987;18:13–23.
[20] Swolfs Y, Gorbatikh L, Verpoest I. Fibre hybridisation in polymer composites: a review. Compos Part A Appl Sci Manuf 2014;67:181–200.
[21] Yu H, Wisnom MR, Potter KD. A novel manufacturing method for aligned discontinuous fibre composites (High Performance-Discontinuous Fibre method). Compos Part A Appl Sci Manuf 2014;65:175–85.
[22] Yu H, Longana ML, Jalalvand M, Wisnom MR, Potter KD. Pseudo-ductility in intermingled carbon/glass hybrid composites with highly aligned discontinuous fibres. Compos Part A Appl Sci Manuf 2015;73:35–44.
[23] Wisnom MR, Czel G, Swolfs Y, Jalalvand M, Gorbatikh L, Verpoest I. Hybrid effects in thin ply carbon/glass unidirectional laminates: accurate experimental determination and prediction. Compos part A Appl Sci Manuf 2016;88:131–9.
[24] Czél G, Wisnom MR. Demonstration of pseudo-ductility in high performance glass-epoxy composites by hybridisation with thin-ply carbon prepreg. Compos Part A Appl Sci Manuf 2013;52:23–30.
[25] Czél G, Jalalvand M, Wisnom MR. Design and characterisation of advanced pseudo-ductile unidirectional thin-ply carbon/epoxy-glass/epoxy hybrid composites. Compos Struct 2016;143:362–70.
[26] Jalalvand M, Czél G, Wisnom MR. Numerical modelling of the damage modes in UD thin carbon/glass hybrid laminates. Compos Sci Technol 2014;94(0):39–47.
[27] Jalalvand M, Czél G, Wisnom MR. Damage analysis of pseudo-ductile thin-ply UD hybrid composites - a new analytical method. Compos Part A Appl Sci Manuf 2015;69:83–93.
[28] Jalalvand M, Czél G, Wisnom MR. Parametric study of failure mechanisms and optimal configurations of pseudo-ductile thin-ply UD hybrid composites. Compos Part A Appl Sci Manuf 2015;74:123–31.
[29] Sihn S, Kim RY, Kawabe K, Tsai SW. Experimental studies of thin-ply laminated composites. Compos Sci Technol 2007;67:996–1008.
[30] Yokozeki T, Aoki Y, Ogasawara T. Experimental characterization of strength and damage resistance properties of thin-ply carbon fiber/toughened epoxy laminates. Compos Struct 2008;82:382–9.
[31] Yokozeki T, Kuroda A, Yoshimura A, Ogasawara T, Aoki T. Damage characterization in thin-ply composite laminates under out-of-plane transverse loadings. Compos Sci Technol 2010;93:49–57.
[32] Saito H, Morita M, Kawabe K, Kanesaki M, Takeuchi H, Tanaka M, et al. Effect

of ply-thickness on impact damage morphology in CFRP laminates. J Reinf Plastics Compos 2011;30:1097–106.
[33] Arteiro A, Catalanotti G, Xavier J, Camanho PP. Notched response of non-crimp fabric thin-ply laminates. Compos Sci Technol 2013;79:97–114.
[34] Arteiro A, Catalanotti G, Xavier J, Camanho PP. Notched response of non-crimp fabric thin-ply laminates: analysis methods. Compos Sci Technol 2013;88:165–71.
[35] Amacher R, Cugnoni J, Botsis J, Sorensen L, Smith W, Dransfeld C. Thin ply composites: experimental characterization and modeling of size-effects. Compos Sci Technol 2014;101:121–32.
[36] Guillamet G, Turon A, Costa J, Renart J, Linde P, Mayugo JA. Damage occurrence at edges of non-crimp-fabric thin-ply laminates under off-axis uniaxial loading. Compos Sci Technol 2014;98:44–50.
[37] Curtis PT, Browne M. Cost-effective high performance composites. Composites 1994;25:273–80.
[38] Naito K, Yang JM, Kagawa Y. Tensile properties of high strength polyacrylonitrile (PAN)-based and high modulus pitch-based hybrid carbon fibers-reinforced epoxy matrix composite. J Mater Sci 2012;47(6):2743–51.
[39] Montagnier O, Hochard C. Optimisation of hybrid high-modulus/high-strength carbon fibre reinforced plastic composite drive shafts. Mater Des 2013;46:88–100.
[40] Tsampas SA, Greenhalgh ES, Ankersen J, Curtis PT. Compressive failure of hybrid multidirectional fibre-reinforced composites. Compos Part a-Applied Sci Manuf 2015;71:40–58.
[41] Amacher R, Cugnoni J, Brunner J, Kramer E, Dransfeld C, Smith W, et al. Towards aerospace grade thin-ply composites. In Proceedings of ECCM17 Conference. Munich, 26–30. June, 2016.
[42] Czél G, Rév T, Jalalvand M, Fotouhi M, Wisnom MR. Demonstration of pseudo-ductility in quasi-isotropic laminates comprising thin-ply UD carbon-epoxy hybrid sub-laminates. In Proceedings of ECCM17 Conference. Munich, 26–30. June, 2016.
[43] Fotouhi M, Suwarta P, Jalalvand M, Czel G, Wisnom MR. Detection of fibre fracture and ply fragmentation in thin-ply UD carbon/glass hybrid laminates using acoustic emission. Compos Part A Appl Sci Manuf 2016;86:66–76.
[44] Czél G, Jalalvand M, Wisnom MR. Pseudo-ductile carbon/epoxy hybrid composites. In Proceedings of ICCM 20 Conference. Copenhagen, 19–24. July, 2015. Paper ID: 3317-1.